

# Algorithm for phasing a segmented mirror

F.Yu. Kanev, V.P. Lukin, and N.A. Makenova

*Institute of Atmospheric Optics,  
Siberian Branch of the Russian Academy of Sciences, Tomsk*

Received July 28, 2003

This paper considers the problem of forming a preset surface of a segmented mirror of a telescope. An iteration algorithm based on analysis of the interference pattern of the radiation reflected from the mirror is used for phasing the mirror segments. At every iteration, the current interferogram is compared with the reference one obtained for the surface of a preset shape. The value of the control goal function, whose minimum is determined in the algorithm, decreases with the decreasing discrepancy between the interferograms. This technique provides for formation of a plane-reflecting surface of the mirror, if the relative displacement of segments does not exceed the half wavelength. It is shown that to extend the range of acceptable displacements, it is necessary to introduce additional sources of radiation of specially chosen wavelengths. In such a case, the dynamic range of the algorithm can be extended up to 30  $\mu\text{m}$ .

## Introduction

Phasing of mirror segments in a telescope is one of the urgent problems of modern optics; the possibility of solving this problem has been widely discussed during recent 10–15 years. Although the algorithms for formation of a reflecting surface are developed and described in the literature, the information for practical implementation of phasing and construction of experimental mockup is obviously insufficient. Therefore, we have constructed a model of an optical system to study the peculiarities of the process of compensation for random displacements of the mirror elements and to formulate the main requirements to the parameters of an experimental setup. Another one problem we have dealt with in this paper is extending the dynamic range of the system, that is, to increase the relative initial displacement, at which segments can be aligned.

## 1. Phasing algorithms. Brief review of the literature

The reflecting surface of the primary mirror of active ground-based telescopes of the class of 8 to 10-m diameter (Subaru, Keck, Gemini, VLT) is formed by a set of segments having about 1-m diameter. This is, likely, the only possible modern technology for creation of big reflectors, which is used in some projects under development, such as the thirty-meter Californian Extra Large Telescope (CELT), fifty-meter Swedish Extremely Large Telescope, and 100-meter Overwhelmingly Large (OWL) telescope.

The Keck telescope primary mirror<sup>1</sup> can be considered an example of such a reflector (Fig. 1). Its reflecting surface is formed from 36 segments, the total aperture diameter is 10 m, with the size of a single element of 0.9 m. The parameters under control in this system are the displacements and tilts of each segment in two perpendicular planes.

After the primary assembling of the telescope, it is needed to perform a series of specialized operations aimed at accurate formation of the shape of a mirror surface. Then the surface should be routinely controlled, and possible deviation from the needed shape, if any, should be compensated for.

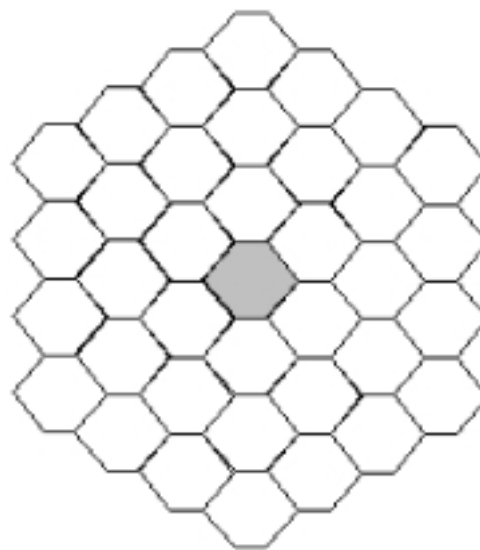


Fig. 1. Segmented mirror of the Keck telescope.

Analysis of the PAMELA (Phase Array Mirror, Extendible Large Aperture) Project described in Ref. 2 showed that the most accurate compensation is possible for random tilts of the segments, while to compensate for the random displacements, it is necessary to provide relevant dynamic range equal to several tens of wavelengths and the accuracy no worse than tenths of wavelength, but this is a rather difficult problem.

One of the phasing versions was proposed in Ref. 3. A recursion algorithm was used to obtain the plane mirror surface. The goal function in this

algorithm was the contrast of the interference pattern of a partially coherent radiation. Based on numerical simulation it was shown in Ref. 3 that phasing permits compensation for the displacements of an element of the initial mirror about 1 μm magnitude. The further increase of the dynamic range is impossible in this method because of the full loss of contrast in the interference pattern.

More advanced phasing methods have recently been proposed and, as was reported in Refs. 1 and 4 to 6, practically implemented at the Keck telescope project. The surface in this case is controlled with the use of interferometric methods, Hartman sensor, and specialized “edge” displacement sensors. As a result, the initial segment displacements about half wavelength can be compensated for by use coherent radiation, and roughly about 300 nm as small if using incoherent radiation.

It should also be noted that neither technology for practical implementation of phasing nor formulation of the requirements to the equipment to be used, which would allow one to begin planning the experiment and realization of the method, can be found in the literature.

## 2. The phasing algorithm proposed. The 2π-problem

In this Section, the problem of phasing is analyzed theoretically. The analysis was performed of how to extend the dynamic range of possible displacements. It is assumed that the Laboratory of Coherent and Adaptive Optics at the IAO (Tomsk, Russia) will experimentally test the algorithm proposed. For that we plan to use two segmented mirrors: one of 4 segments and the other of 18 segments.

In our theoretical study, we used the model of radiation propagation through a linear medium (vacuum). The beams of coherent generated by laser sources were reflected from two neighboring elements and focused at a point by beam-deflecting mirrors. The interface of the program developed for numerical simulation is shown in Fig. 2 along with the ray paths and the experimental geometry. The simulation was performed for a mirror with only two segments, since it is assumed that the increase of the number of mirror elements introduces no principal changes into the phasing process.

For the interference pattern recorded in the observation plane, the intensity of maxima and minima for the plane waves is determined by the following equations<sup>7</sup>:

$$I_{\max} = I_1 + I_2 + 2\sqrt{I_1 I_2} \cos(\Delta\phi),$$

$$I_{\min} = I_1 + I_2 - 2\sqrt{I_1 I_2} \cos(\Delta\phi).$$

Here  $I_1$  and  $I_2$  are the intensities of the interfering waves;  $\Delta\phi$  is the phase shift due to the propagation path difference. The conditions for maximum and minimum of the interference pattern are,

$$|\Delta\phi| = 0, 2\pi, 4\pi, \dots$$

and

$$|\Delta\phi| = \pi, 3\pi, \dots$$

For the optical arrangement shown in Fig. 2a, the phase shift  $\Delta\phi$  can be determined as

$$\Delta\phi = 2\pi\Delta z/\lambda, \tag{1}$$

where  $\lambda$  is the radiation wavelength;  $\Delta z$  is the relative displacement of the segments. This means that the positions of interference maxima and minima depend on the relative displacement of the segments  $\Delta z$ , that is, the interference fringes shift as variation of  $\Delta z$ . Therefore, for phasing we used the algorithm, which determined the minimum of  $\Delta z$  from deviation of the interferogram obtained for displaced segments from the interferogram of a plane surface.

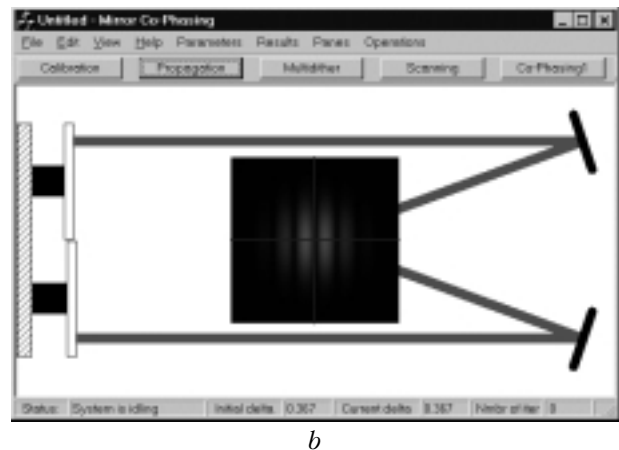
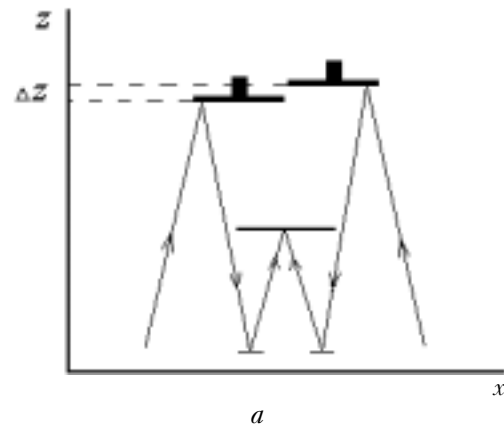


**Fig. 2.** Phasing of segmented mirror elements. The figure shows the ray paths in simulated optical layout (a) and the interface of the program used (b).

The minimum of  $\Delta z$  was found using the aperture sensing algorithm,<sup>8</sup> in which only one coordinate was used for control:

$$z_{n+1} = z_n + \alpha \frac{dJ(z)}{dz}, \tag{2}$$

where  $z_{n+1}$ ,  $z_n$  are the displacements of a segment at the  $(n + 1)$ th and  $n$ th iterations;  $\alpha$  is the iteration

step;  $J(z)$  is the control goal function. The second segment was assumed fixed and  $z = 0$  for it.

In this problem, the criterion

$$J_{\text{cor}}(z) = \frac{\langle I_1(x,y)I_2(x,y) \rangle}{\langle I_1(x,y)I_1(x,y) \rangle}, \quad (3)$$

was taken as a goal control function. The value of this criterion is determined by correlation between the interferogram at the current step of the iteration process and the reference obtained at the zero relative displacement of the elements. In Eq. (3)  $I_1(x,y)$  is the intensity distribution of the reference light field;  $I_2(x,y)$  is the intensity distribution for the interferogram of the mirror with displaced segments. The closer the agreement between the reference and the  $n$ th interference patterns, the larger is the criterion (3). At full coincidence,  $J_{\text{cor}}(z) = 1$  and it decreases with the increasing discrepancy between the interference patterns.

To implement the aperture sensing, it is also possible to use the energy criterion, whose value is proportional to the energy of radiation falling within the narrow band at the center of the observation plane. Our numerical experiments have shown that introduction of this criterion does not change the accuracy and speed of the algorithm developed and does not lead to solution of the  $2\pi$ -problem.

At the initial stage of the study, the segments were phased at the wavelength  $\lambda = 0.8 \mu\text{m}$ , that is, roughly equal to the red light wavelength.

The numerical experiments showed that convergence of the phasing algorithm is determined by the initial  $\Delta z$ , namely, at  $\Delta z < \lambda/2$  the mirror surface obtained as a result of control is plane ( $\Delta z = 0$ ), while at  $\Delta z > \lambda/2$  the aperture sensing leads to the increase of the relative displacement between segments.

The data characterizing the compensation for the initial displacement of the mirror elements in a more detail are shown in Figs. 3 and 4, which depict the variation of the criterion  $J_{\text{cor}}(z)$  and the relative displacement of the segments  $\Delta z$  in the process of aperture sensing. One can see that in both situations considered the criterion  $J_{\text{cor}}(z)$  increases identically, while the displacement of the elements increases in one case and decreases in the other.

Figures 3 and 4 can be explained using Eq. (1), according to which the relative displacement of the segments by one wavelength leads to the phase shift of the beams by  $2\pi$ . As known,<sup>7</sup> the interferogram does not change at such phase shift, that is, the current distribution of the light field is equal to the reference one, and the criterion (3) is equal to unity. The minimum of the criterion corresponds to the  $\lambda/2$  shift, and two identical maxima are located to the right and to the left of this point. The aperture sensing algorithm shifts the segments toward the left maximum ( $\Delta z \rightarrow 0$ ), if the initial displacement is less than  $\lambda/2$ , and toward the right one ( $\Delta z \rightarrow \lambda$ ), if the initial displacement  $\Delta z > \lambda/2$ . Therefore, in Fig. 4

the resulting displacement in the first case is zero, and in the second case it is  $0.8 \mu\text{m}$ .

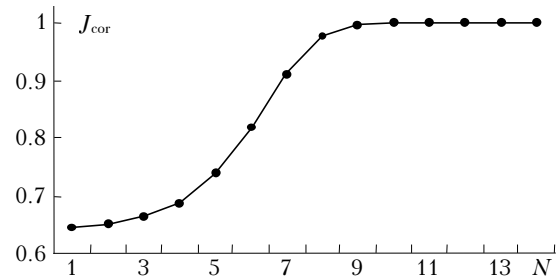


**Fig. 3.** Variation of the correlation criterion of focusing  $J_{\text{cor}}$  at aperture sensing (initial displacements of the segments were set  $\Delta z = 0.367$  and  $0.433 \mu\text{m}$ ; the wavelength  $\lambda = 0.8 \mu\text{m}$ , the curves coincided in both of the cases).  $N$  is the number of the iteration step.

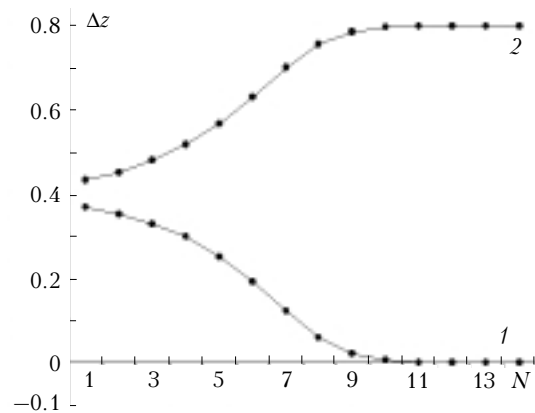


**Fig. 4.** Variation of the relative displacement of mirror segments  $\Delta z$  in the process of aperture sensing (wavelength  $\lambda = 0.8 \mu\text{m}$ ): initial displacement  $\Delta z = 0.367 \mu\text{m}$  (curve 1) and  $0.433 \mu\text{m}$  (2);  $N$  is the number of the iteration step.

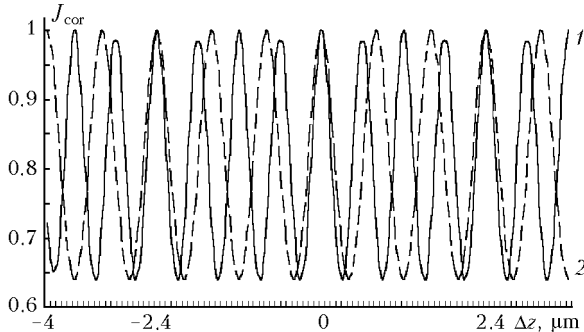
The above description of the control process shows that this problem involves the so-called  $2\pi$ -problem, which restricts the maximum allowable initial displacement of the segments to  $\lambda/2$  while actually, to even smaller values, since measurements of the criterion have a finite accuracy, and at  $\Delta z \approx \lambda/2$  the area of uncertainty arises, in which the algorithm gives the resulting displacement equal to zero or  $\lambda$  with the same probability.

### 3. Extension of the dynamic range of the algorithm

The range allowed for the initial displacements can be extended by introducing additional wavelength into the control algorithm. Thus, Figure 5 depicts the criterion  $J_{\text{cor}}$  [defined by Eq. (3)] calculated at variation of the relative displacement of the segments for the wavelengths  $\lambda = 0.6$  and  $0.8 \mu\text{m}$ .

Curves 1 and 2 were obtained in the following way: first a small segment displacement was set, then interferograms were recorded at two wavelengths, the current interferograms were compared with the

reference one, two values of the criterion  $J_{cor}$  were calculated, and then a new small displacement was set, and the process was repeated for the entire range of the coordinate  $z$  variation.



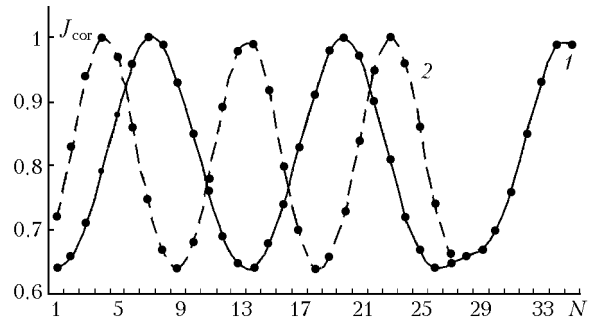
**Fig. 5.** Dependence of the correlation criterion  $J_{cor}$  on the relative displacement of the mirror segments  $\Delta z$ :  $\lambda = 0.6$  (curve 1) and  $0.8 \mu\text{m}$  (curve 2).

Figure 5 shows that the physical displacement of the segments by the same value gives different phase shifts for different wavelengths; therefore, the maxima of the criterion coincide only at  $\Delta z = 0$  and  $\Delta z = 2.4$  ( $-2.4$ )  $\mu\text{m}$ . Note that 2.4 is the least common multiple of 0.6 and 0.8, and the phase shifts in this case are, respectively,  $8\pi$  and  $6\pi$ . For these points, the interferograms coincide with the reference ones. At other points, the maxima of  $J_{cor}$  at the two wavelengths are different. For example, at  $\Delta z = 0.8 \mu\text{m}$   $J_{cor} = 1$  for the red light, while for  $\lambda = 0.6 \mu\text{m}$   $J_{cor} < 1$ , and the interferograms are different.

This allows us to construct the following iteration algorithm of phasing. At the initial stage, aperture sensing is off, and the relative position of the segments is changed within the allowed range of displacements. At every next step, the interference patterns for the two wavelengths are recorded, and the criteria  $J_{cor1}$  and  $J_{cor2}$  are calculated for each pattern. The rough identity of  $J_{cor1}$  and  $J_{cor2}$  means that the algorithm is near the global maximum, and the scanning is stopped. The final value of the displacement does not provide the position of the extreme, so at this point it is worth turning the aperture sensing algorithm on, and it finds the maximum with high accuracy. The functioning of the algorithm is illustrated in Figs. 6 and 7.

The scanning is performed at two wavelengths, and at the 27th iteration the difference between the criteria becomes small enough (see Fig. 6), scanning is stopped, and the aperture sensing algorithm at the wavelength of  $0.8 \mu\text{m}$  starts. The control is completely stopped on achieving the maximum of the goal function. The corresponding change in the relative displacement of the segments  $\Delta z$  is shown in Fig. 7 (curve 1). The initial displacement was  $2 \mu\text{m}$ , and the resulting one is nearly zero. The maximum allowable displacement, at which phasing is possible, was equal to  $2.34 \mu\text{m}$  in this algorithm. At a larger initial

displacement ( $4 \mu\text{m}$ , curve 2 in Fig. 7) the resulting displacement of the segments is  $2.4 \mu\text{m}$ , which corresponds to the point of coincidence of the criteria. Thus, introducing the second wavelength into the algorithm has significantly extended the range of displacements, at which the mirror can be phased (from  $0.36$  to  $2.34 \mu\text{m}$ ).



**Fig. 6.** Variation of the correlation criterion  $J_{cor}$  in the algorithm of phasing of mirror segments:  $\lambda = 0.8$  (curve 1) and  $0.6 \mu\text{m}$  (curve 2).

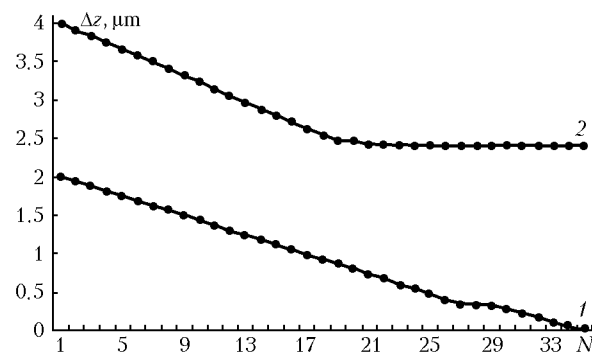


**Fig. 7.** Variation of the relative displacement of mirror segments in the phasing algorithm: the initial displacement of  $2.0$  (curve 1) and  $4.0 \mu\text{m}$  (curve 2).

Further extension of the range can be achieved by proper selection of the wavelengths of the interfering beams and by introducing third wavelength. The data characterizing the allowed ranges of the displacements are tabulated below.

Allowable ranges of displacements			
$\lambda_1, \mu\text{m}$	$\lambda_2, \mu\text{m}$	$\lambda_3, \mu\text{m}$	$\Delta z, \mu\text{m}$
0.8	—	—	0.36
0.6	—	—	0.26
0.6	0.8	—	2.34
0.7	0.8	—	5.55
0.6	0.7	0.8	33.4

Note.  $\Delta z$  is the maximum acceptable displacement, at which phasing of the mirror surface is still possible;  $\lambda_i$  are the control wavelengths.

Thus, at  $\lambda_1 = 0.7$  and  $\lambda_2 = 0.8 \mu\text{m}$  the least common multiple is 5.6, and the maximum displacement of the segments that can be compensated for is  $5.55 \mu\text{m}$ .

Finally, the displacement range can be further extended whilst incorporating third wavelength into the control. Numerical experiments showed that at  $\lambda_1 = 0.6$ ,  $\lambda_2 = 0.7$ , and  $\lambda_3 = 0.8 \mu\text{m}$ , phasing can be accomplished at  $\Delta z = 33.4 \mu\text{m}$ .

In general, the results presented suggest that the algorithm of phasing the segmented mirror surface developed provides a rather good accuracy and a wide dynamic range.

### References

1. G.A. Chanan, J.E. Nelson, and T.S. Mast, Proc. SPIE **628**, 466–470 (1986).
2. J.M. Becher, Ker-Li Shu, and S. Shaklan, Proc. SPIE **628**, 102–106 (1986).
3. K.N. Shrader, R.H. Fetner, M.J. Balas, and R.S. Erwin, Proc. SPIE **4849**, 146–157 (2002).
4. G.A. Chanan, J.E. Nelson, T.S. Mast, P. Wizinovich, and B. Schaefer, Proc. SPIE **2198**, 1139–1150 (1994).
5. J.M. Geary, *Introduction to Wavefront Sensors* (SPIE Press, 1995), Vol. TT18, 215 pp.
6. A.D. Gleckler, B.L. Ulich, C. Sheppard, and E.K. Conklin, in: *Greenbank Telescope Project. Related Experience and Capabilities*: Report of Kaman Aerospace Corporation (1990), pp. 98–108.
7. M. Born and E. Wolf, *Principles of Optics* (Pergamon, New York, 1959).
8. M.A. Vorontsov and V.I. Shmalgauzen, *Principles of Adaptive Optics* (Nauka, Moscow, 1985), 335 pp.